Study of Structural and Ferroelectric Properties of Dy doped $BiFeO_3$–$PbTiO_3$ solid solution

Manoj Baloni[1,*], Ram Chhavi Sharma[2,], Anand Singh Rana[1], Anita Manori Dhyani[1]

[1]*Department of Physics, SGRR(PG) College Dehradun,Uttarakhand, India*

[2]*Department of Physics, SGT University,Gurugram, Haryana, India*

*Corresponding Author: Manoj Baloni

Department of Physics

SGRR(PG) College Dehradun(UK)

Email: manojbaloni@rediffmail.com

Article Info
Page Number: 847-855
Publication Issue:
Vol. 72 No. 1 (2023)

Article History
Article Received: 15 October 2022
Revised: 24 November 2022
Accepted: 18 December 2022

Abstract

Solid state reaction method was used to fabricate Dy modified $BiFeO_3$-$PbTiO_3$ i.e $0.65Bi_{1-x}Dy_xFeO_3$-$0.35PbTiO_3$ with x = 0.15 and 0.20 solid solution. The structural analysis based on X-ray diffraction (XRD) data ensures the transition from rhombohedral to tetragonal phase of solid solutions. SEM micrographs revealed a dense microstructure with non-uniform grains, which alters the ferroelectric properties of these solid solutions. Electric field dependent polarization (PE-hysteresis) loops confirm the ferroelectric nature of the compounds. Saturated ferroelectric loops with low remnant polarization have been observed which may be related to the ability of samples for various electronics device applications.

Keywords: $BiFeO_3$, XRD, SEM, PE-hysteresis, Remnant polarization.

1. Introduction:

Energy storage materials that are paired with both a high power density and a large energy storage density become increasingly crucial due to the rising need for portable electronics, power electronics and other devices [1]. Multiferroic materials, which integrate structural, electric, and magnetic order characteristics to produce multifunctional devices, have recently attracted attention [2,3]. Because multiferroic composites have a substantially higher magnetoelectric (ME) effect than single phase materials, they have attracted researchers' attention for a range of device applications, including actuators, sensors, memory devices, etc [4,5]. One of the most thoroughly investigated materials is bismuth ferrite, or $BiFeO_3$ (BFO), which is a single phase multiferroic at ambient temperature and has a ferroelectric Curie point at 1098 K and an antiferromagnetic-paramagnetic transition temperature of 640 K [6]. Due to the high temperature of ferroelectric and antiferromagnetic ordering, BFO, a common single phase multiferroic compound, has attracted a lot of attention among other multiferroic materials. [7]. The distorted perovskite structure for BFO with rhombohedral crystal symmetry and the space group *R3c* has been confirmed using X-ray diffraction (XRD) and neutron diffraction techniques [8,9]. The ferromagnetism in BFO is caused by the partially filled 3d-orbitals of the Fe3+ ion, while the ferroelectricity is caused by the stereochemical activity of the Bi lone electron pair. [10,11].

Aside from that, BFO has some inherent drawbacks, such as secondary phase formation, high leakage current, and a lack of structural distortion. One disadvantage is the low spontaneous saturation magnetization, which is caused by spin helical ordering of magnetic moments, which suppresses magneto-electric coupling between ordered parameters, i.e. ferroelectricity and magnetism [12-14]. Researchers have experimented with doping different rare earth elements onto the perovskite material BFO in order to get around these restrictions and also attempted to create composites using other perovskite materials [15-18]. It is challenging to demonstrate well-saturated ferroelectric P-E loops due to the low resistivity of bulk BFO samples. The Fe ions' varied oxidation states, such as Fe^{3+} and Fe^{2+}, as well as anion vacancies, which negatively impact both magnetic and ferroelectric properties, are the main causes of the BFO sample's low resistivity [19,20]. The Nd^{3+} substitution in BFO has also been reported by Gaur et al. to reduce leakage current and eliminate secondary phases [21]. Due to its increased multiferroic properties, ceramic samples made of $BiFeO_3$-$PbTiO_3$ (BF-PT) have attracted a lot of attention from researchers. By substituting La in 0.6BF-0.4PT, Cotica et al. reported controlling the crystalline phase and ferroelectric behavior [22]. In Gd^{3+} modified 0.8BF-0.2PT and Sm^{3+} doping to 0.8BF-0.2PT solid solutions, Sahu et al. showed improved resistivity and ferroelectric behavior above room temperature [23,24].

Numerous literary works have recently discussed the development of composites of perovskite-type materials, such as $PbTiO_3$ or $BaTiO_3$,which enhance multiferroic characteristics [25,26]. By measuring ferroelectric loops and the magnetoelectric coefficient, Pradhan et al. investigated the improve multiferroic characteristics of a La-modified $(BiFeO_3)_{1-x}(PbTiO_3)_x$ system [27]. Rare earth element substitution, as stated above, has definitely had an impact on the structural, dielectric, ferroelectric, and ferromagnetic properties of BFO and BF-PT ceramics. $PbTiO_3$, or PTO, is used in this work because of its high polarisation and dielectric constant ferroelectric material, which settles the perovskite phase of the composite and also generates an MPB with BFO due to the distinction in crystal symmetry between PTO and BFO. Additionally, we created a BF-PT solid solution to reduce leakage current and enhance the functional qualities of BFO. The objective of the current study was to synthesize and investigate the structural, ferroelectric, and piezoelectric properties of $0.65Bi_{1-x}Dy_xFeO_3$-$0.35PbTiO_3$ $(BDFPT)_x$ solid solutions with x = 0.15, and 0.20.

2. Experimental Details:

A solid state reaction technique was used to synthesize $0.65Bi_{1-x}Nd_xFeO_3$-$0.35PbTiO_3$ solid solutions with x= 0.15 and 0.20. Analytical grade high purity oxides of Bi_2O_3, Dy_2O_3, Fe_2O_3, PbO, and TiO_2 were first combined in stoichiometric proportions and thoroughly ground for 4 hours in the presence of acetone in an agate mortar. The powders were then calcined for 2 hours in furnance at 820 °C. After calcination, the samples were mixed with polyvinyl alcohol (PVA) (2 wt%) and ground in the agate mortar for another 2 hours. Pellet specimens of 1 mm thickness and 8 mm diameter were prepared from blended powders of various compositions squeezed into circular discs with a pressure of 1.5×10^8 Pascal and sintered at 820^{oC} for 2 hours. In a Bruker D8 Advance X-ray diffractometer operating at room temperature, CuK radiation with a wavelength of 1.5406Å was utilized to analyze the phase formation and crystal structure of the annealed powders. A scanning electron microscope (Carl Zeiss EVO18) with a 20KeV electron beam intensity was used to analyze the surface morphology of synthesized samples. A Ferroelectric loop tracer(aiXACCT Systems GmbH aixPES) was used to examine the Polarization Hysteresis Loops and the piezoelectric characteristics of shrunk, publishable pellets coated with high conducting silver paste of various samples.

Results and Discussion:

3.1 ***XRD Studies:*** The XRD pattern from the powder sample was used to determine the crystal structures related to the $(BDFPT)_x$ samples with x = 0.15, and 0.20. The XRD pattern of $(BDFPT)_x$ with x = 0.15, and 0.20 in the 20°-60° range are shown in Figure 1. In contrast to $BiFeO_3$, which has rhombohedral crystal structure with the space group *R3c*, $PbTiO_3$ has tetragonal symmetry with the space group *P4mm* [7,28]. Along with the XRD peaks corresponding to $BiFeO_3$ with increasing Dy doping, it is observed that new peaks also appear which are caused by the tetragonal phase of $PbTiO_3$ concentration as illustrated by T in [Fig.1]. The XRD pattern further suggests that the Dy dopant substituted at the Bi site of BFO helps to reduce the strong diffraction peak (104) associated with BFO phase in the doped samples in order to get improved $PbTiO_3$ phase. Additionally, it is observed that the solid solutions change from its crystalline state to an amorphous one by steadily spreading the diffraction peaks with increasing doping. The results show a considerable effect of doping at the Bi^{3+} site location.

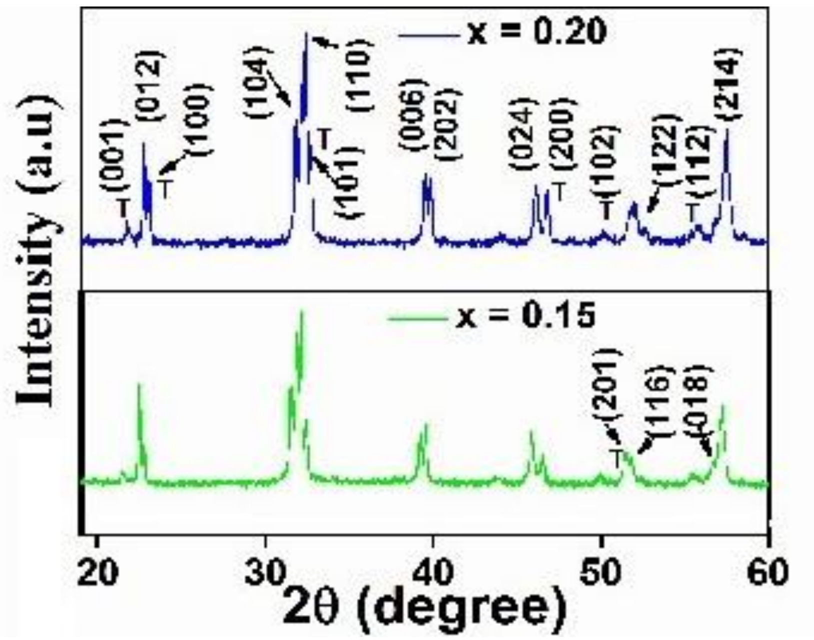

Figure 1. X-ray diffraction pattern of $(BDFPT)_x$ with x = 0.15 and 0.20.

The lattice parameters of $(BDFPT)_x$ samples corresponding to rhombohedral structure (equivalent hexagonal) are calculated using the formula $\frac{1}{d^2} = \frac{4}{3}\left(\frac{h^2+hk+k^2}{a^2}\right) + \frac{l^2}{c^2}$, where miller indices (hkl) of the two highest intensity peaks of the XRD pattern, namely (012) and (110) are used. While the lattice parameters corresponding to tetragonal structure are determined using the formula $\frac{1}{d^2} = \left(\frac{h^2+k^2}{a^2}\right) + \frac{l^2}{c^2}$, where the miller indices (hkl) of the two highest intensity peaks of the XRD pattern, namely (100) and (101), are taken. The interplaner spacing (d) is calculated by the equation $2dsin=n\lambda$, where n is the order of x-ray spectra and λ is the x-ray wavelength (1.5406Å). The lattice constants and cell volume for rhombohedral and tetragonal structures are displayed in Table 1. The variations in lattice characteristics unambiguously show that Dy intrusion significantly affects the Bi site. Similar findings have been observed in earlier investigations on rare earth doped BT-PT binary systems. [29,30].

Table 1.

Lattice Parameters and Average Grain size of $(BDFPT)_x$ ceramics with x = 0.15 and 0.20 compositions.

Composition x	**Crystal Structure**	**Lattice Parameters**	**Average Grain Size (µm)**
0.15	Rhombohedral (*R3c*)	a =5.5589Å b =5.5589Å c =13.78 Å	1.25
	Tetragonal (*P4mm*)	a = 3.8850 Å b = 3.8850 Å c =4.1070 Å	
0.20	Rhombohedral (*R3c*)	a =5.5520Å b =5.5520Å c =13.25 Å	1.14
	Tetragonal (*P4mm*)	a = 3.8804 Å b = 3.8804 Å c =4.1022 Å	

3.2. *Morphological Studies:* SEM was used to examine the surface morphology of sintered samples, and Figure 2 shows the surface morphology of a $(BDFPT)_x$ solid solutions with varied x components. Well-developed grains were present in all processed samples. The oblate cuboid structure of the granular grains in the SEM micrograph has a covering of grains with spherical grain shapes. In the micrograph, the surface grain distribution is uniformly dense. ImageJ software was used to determine the average grain size of the produced samples, as shown in Table 1. The average grain size is discovered to drop from 1.25µm to 1.14µm with increased Dy content. The levels of oxygen vacancies and ion transport rates have an impact on grain formation [31]. Pure $BiFeO_3$ has a significant amount of oxygen vacancies due to the high volatility of Bi. Dy has a higher valence than Fe, which decreases the creation of oxygen vacancies and, in turn, decreases the average particle size.

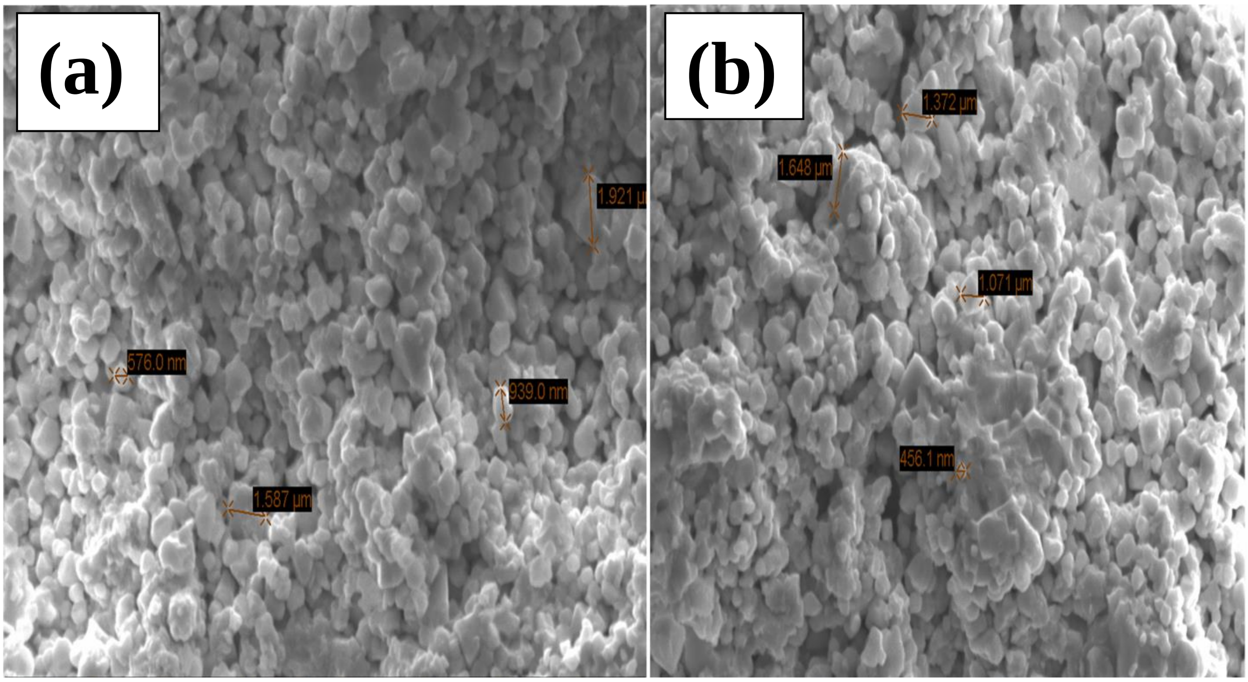

Figure 2. SEM images of $(BDFPT)_x$ solid solutions (a) $x = 0.15$, (b) $x = 0.20$.

3.3. *Ferroelactric properties:* The ferroelectric behaviour of BFO is restricted by the conductive behaviour, which prevents the application of higher fields [13]. The primary cause of the conductive behaviour in BFO compound is the high leakage current [6]. It is observed that the Nd^{3+} ion reduces the leakage current in Nd doped $BiFeO_3$-$PbTiO_3$ in compare to binary $BiFeO_3$-$PbTiO_3$ systems [32,33]. Polarization versus electric field plots (P-E loop) of $(BDFPT)_x$ with $x = 0.15$,and 0.20 measured at 30 Hz at room temperature are shown in Figure 3. It is observed that the saturation polarization (P_s) and remnant polarization (P_r) are larger for $x = 0.15$ and then get smaller as the Dy concentration rises as illustrates in Table 4. The similar ferroelectric phenomenon was observed by Sahu et al. in rare earth ion (Sm) modified $BiFeO_3$–$PbTiO_3$ solid solutions [23]. The decrease in residual polarization may be due to structural distortions in produced compounds as well as differences in the ionic radii of Dy^{3+} and Fe^{3+} ions. Ferroelectricity is caused by the ferroelectric distortion of the Ti (3d) orbital and the O (2p) orbital of $PbTiO_3$, as well as the Bi ($6s^2$) lone pair and the O (2p) orbital of the $BiFeO_3$ crystal. The lattice parameter modification caused by Dy^{3+} intrusion in the BFO compound, which also distorts the tetragonal unit cell at the morphotropic phase boundary (MPB) region effect the polarization.

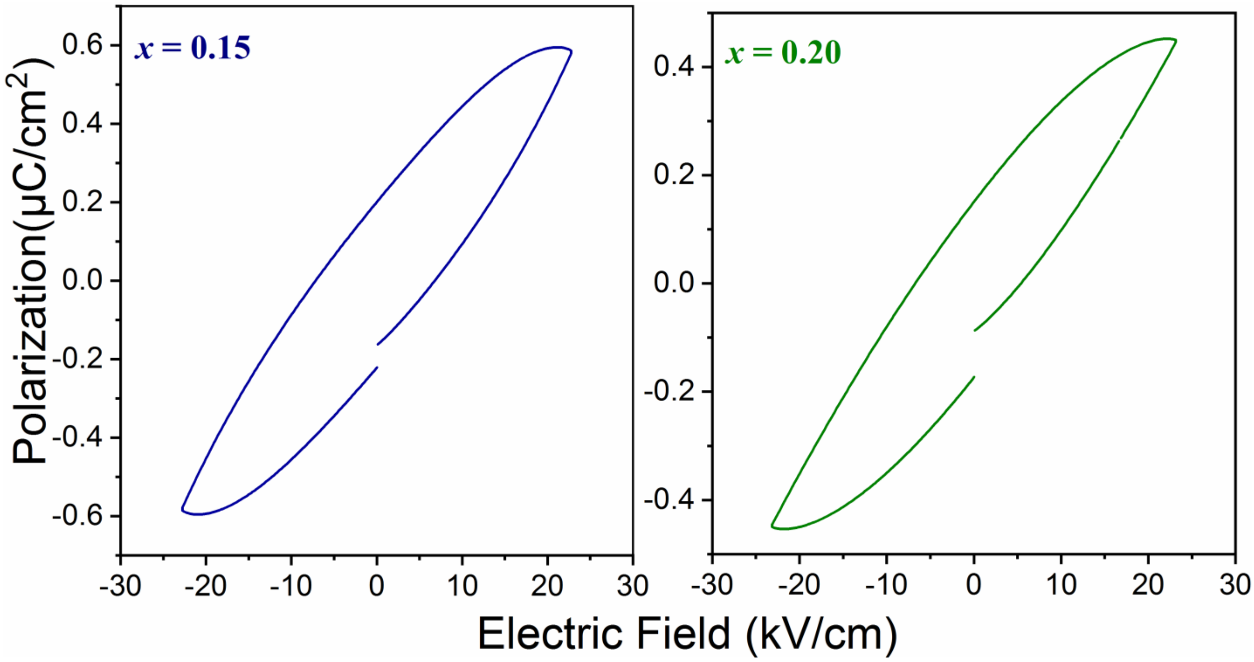

Figure 3. P-E loops of (BDFPT)$_x$ samples for x = 0.15 and x = 0.20 compositions.

In addition, various studies have shown that oxygen vacancies in materials have an impact on remnant polarization [34,35]. The high-temperature sintering process results in the formation of oxygen and lead vacancies, mainly as a result of PbO evaporation and these vacancies create defect dipoles [36]. The induced polarization vector produced by these dipoles requires more energy to reorient in the field direction, and the restoring force established as a result of the constant polarization vector favors the domains returning to their initial state, resulting in a decrease in remnant polarization. Kumar et al. [37] observed similar correlations between remnant polarization and oxygen vacancies in Sr doped $BiFeO_3$-$PbTiO_3$ ceramics. Additionally, all of the produced samples only cover a tiny area in hysteresis loops, which may be connected to the ability of the samples to store energy [38].

Table 4. Saturation polarization (P_s), remnant polarization (P_r), and coercive field (E_c) for (BDFPT)$_x$ samples for x = 0.15 and x = 0.20 compositions

Composition (x)	P_s(μC/cm^2)	P_r (μC/cm^2)	E_c (kV/cm)
0.15	0.5871	0.2119	7.0790
0.20	0.4537	0.1627	6.1805

Conclusions:

Effective synthesis of $0.65Bi_{1-x}Dy_xFeO_3$-$0.35PbTiO_3$ solid solutions for x = 0.15 and x = 0.20 compositions was accomplished using the conventional solid-state reaction technique. XRD investigation suggests a tetragonal (*P4mm*) crystal structure as Dy doping increased, along with a rhombohedral crystal structure with the *R3c* space group. Morphological Studies indicates the reduction of grain size of prepared samples from 1.25µm to 1.14µm. The reduction in lattice parameters clearly shows that Dy doping has a significant impact on the structural properties. Low remnant polarization and a coercive field with increasing doping were found in the ferroelectric investigation, which may be related to the samples' ability to store energy. This makes the material a desirable option for upcoming applications.

Acknowledgments

The author Manoj Baloni would like to express his appreciation to the administrators of HNB Garthwal Central University Srinagar, Uttaranchal University Dehradun and SGT University Gurugram Haryana for providing lab facilities for samples characterization.

References

1. K. Yu, Y. Niu, Y. Zhou, Y. Bai, H. Wang, Nanocomposites of surface-modified BaTiO3 nanoparticles filled ferroelectric polymer with enhanced energy density, J. Am.Ceram. Soc. 96 (2013) 2519–2524.
2. M. Fiebig, Th. Lottermoser, D.Frolich, A.V.Goltsev and R.V. Pisarev, Observation **of coupled magnetic and electric domains, Nature. 419 (2002) 818-820.**
3. Y.-H. Chu et al., Electric-field control of local ferromagnetism using magneto electric multiferroic. Nature Mater. 7(2008) 478–482.
4. S.W. Cheong and M. Mostovoy, Multiferroics: a magnetic twist for ferroelectricity,Nat. Mater. 6 (2007) 13-20.
5. M. Fiebig, Revival of the magnetoelectric effect, J. Phys. D Appl. Phys. 38 (2005) R123.
6. F. Kubel and H. Schmid, Structure of a ferroelectric and ferroelastic monodomain crystal of the perovskite $BiFeO_3$, Acta Crystallogr. B 46 (1990) 698.
7. M. Cebela, D. Zagorac, K. Batalovic, J. Radakovic, B. Stojadinovic, V. Spasojevic andR. Hercigonja, BiFeO3 Perovskites: A multidisciplinary approach to multiferroics, Ceram. Int. 43 (2017) 1256-1264.
8. C. Michel, J. M. Moreau, G. D. Achenbach, R. Gerson and W. J. James, The atomic structure of $BiFeO_3$, Solid State Commun.9 (1969) 701.
9. P. Fischer, M. Polomska, I. Sosnowska and M. Szymanski,Temperature dependence of the crystal and magnetic structures of $BiFeO_3$, J. Phys. C 13 (1980) 1931.
10. P. K. Siwach, H. K. Singh, J. Singh and O. N. Srivastava, Anomalous ferromagnetism in spray pyrolysis deposited multiferroic $BiFeO_3$ films, Appl. Phys. Lett. 91 (2007) 2503.
11. V. A. Khomchenko, M. Kopcewicz, A. M. L. Lopes, Y. G. Pogorelov, J. P. Araujo, J. M. Vieira and A. L. Kholkin, Intrinsic nature of the magnetization enhancement in hetero valently doped $Bi_{1-x}A_xFeO_3$ (A= Ca, Sr, Pb, Ba) multiferroics, J. Phys. D, Appl. Phys. 41 (2008) 102003 .
12. V.R. Palkar, J. John and R. Pinto, Observation of saturated polarization and dielectric anomaly in magnetoelectric $BiFeO_3$ thin films, Appl. Phys. Lett. 80 (2002) 1628.
13. G. Catalan, J.F. Scott, Physics and applications of bismuth ferrite.Adv. Mater. 21 (2009) 2463– 2485.

14. C. Ederer, N.A. Spaldin, Weak ferromagnetism and magnetoelectric coupling in bismuth ferrite. Phys. Rev. B 71 (2005) 060401-1-4.
15. X. Jiang, Y. Jiang, J. Chen, D.Hu, J. Xing, B. Wang and J. Cheng, Structural and multiferroic characterization of $BiFeO_3$-$PbTiO_3$ based solid solution with an extra phase, Ceram. Int. 44 (2018) 23315-23319.
16. R. Ranjan and K. A. Raju, Unconventional mechanism of stabilization of a tetragonal phase in the perovskite ferroelectric $(PbTiO_3)_{1-x}(BiFeO_3)_x$, Phys. Rev. B 82 (2010) 054119.
17. P. Suresh and S. Srinath, Observation of high coercivity in multiferroic lanthanum doped $BiFeO_3$. J.Alloys.Compd,554 (2013) 271–276.
18. W. Hu, Y. Chen, H. Yuan, G. Li, Y. Qiao, Y. Qin and S. Feng, Structure, Magnetic, and Ferroelectric Properties of $Bi_{1-x}Gd_xFeO_3$ Nanoparticles, J. Phys. Chem. C. 115 (2011) 8869–8875.
19. G. Catalan, J. F.Scott, Physics and applications of bismuth ferrite. Adv Mater 21 (2009) 2463–2485.
20. J.R. Cheng et al., Structural and dielectric properties of Ga-modified BiFeO3–PbTiO3 crystalline solutions. J Appl Phys 94 (2003) 5153–5157.
21. A. Gaur et al., Structural, optical and magnetic properties of Nd-doped $BiFeO_3$ thin films prepared by pulsed laser deposition. Phys B Condensed Matter 406 (2011) 1877–1882.
22. F.L. Cotica et al., Ferroic states in La doped $BiFeO_3$–$PbTiO_3$ multiferroic compounds. J Appl Phys 111(2011)114105–114110.
23. T. Sahu and B. Behera Investigation on structural, dielectric and ferroelectric properties of samarium-substituted $BiFeO_3$–$PbTiO_3$ composites. J Adv Dielectr 7 (2017) 1750001-6.
24. T. Sahu, A.K. Patra and B. Behera, Effect of Gadolinium doping on structural, ferroic and electrical properties of $0.8BiGd_xFe_{1-x}O_3$–$0.2PbTiO_3$ (x = 0.00, 0.05, 0.10, 0.15 and 0.20) composites. J Alloys Compd 695 (2017) 2273–2284.
25. M. Shariq, D. Kaur and V.C. Chandel, Structural, magnetic and optical properties of mulitiferroic $(BiFeO3)_{1-x}(BaTiO3)_x$ solid solutions. Chin.J. Phys. 55 (2017) 2192–2198.
26. W. H. Sakamoto et al., Synthesis and characterization of BiFeO3−PbTiO3 thin films through metalorganic precursor solution. Jpn. J. Appl. Phys. 45 (2006) 47315–7320.
27. S.K. Pradhan et al.,Structural and electrical properties of lead reduced lanthanum modified $BiFeO_3$−$PbTiO_3$ solid solution. J. Mater. Sci. Mater. Electron. 28 (2017) 1186–1198.
28. Z. Yao, Y. Liu, Z. Song, Z.Wang, H. Hao, M. Cao, Z. Yu, and H.Liu, Structure and electrical properties of ternary $BiFeO_3$ -$BaTiO_3$-$PbTiO_3$ high-temperature piezo ceramics, J. Adv. Cream.1 (2012) 227-231.
29. J. Cheng, N. Li and L. E. Cross, structural and dielectric properties of Ga-modified $BiFeO_3$-$PbTiO_3$ crystalline solution, J. Appl. Phys. 94 (2003) 5153-5157.
30. M. Baloni et al., Effect of Nd doping on structural, dielectric, magnetic and ferroelectric properties of $0.8BiFeO_3$-$0.2Pb\ TiO_3$ solid solution, J. Alloys Compd. 905 (2022) 164228.
31. A. Brinkman, M. Huijben, M. van Zalk, J. Huijben, U. Zeitler, J.C. Maan, W.G. vander

32. Wiel, G. Rijnders, D.H.A. Blank and H. Hilgenkamp, Magnetic effects at the interface between non-magnetic oxides, Nat. Mater. 6 (2007) 6493–496.
33. M. Baloni et al., Structural modification and evaluation of dielectric,magnetic and ferroelectric properties of Nd- modified BiFeO3 – PbTiO3 multiferroic ceramics, Ferroeletric 589 (2022) 161-176.
34. S. Kumar, et al., Correlation between multiferroic properties and processing parameters in $NdFeO_3$–$PbTiO_3$ solid solutions, J. Alloys. Compd. 764 (2018) 824–833.
35. B.L. Cheng, T.W. Button and M. Gabbay, Oxygen vacancy relaxation and domain wall hysteresis motion in cobalt-doped barium titanate ceramics, J. Am. Ceram. Soc. 88 (2005) 907–911.
36. W.L. Warren, K. Vanheusden, D. Dimos, G.E. Pike and B.A. Tuttle, Oxygen vacancy motion in perovskite oxides, J. Am. Ceram. Soc. 79 (1996) 536–538.
37. A. Chandrasekaran, D. Damjanovic, N. Setter and N. Marzari, Defect ordering and defect-domain-wall interactions in $PbTiO_3$: a first-principles study, Phys. Rev. B. 88 (2013) 214116.
38. N. Kumar, B. Narayan , A. K. Singh and S. Kumar Enhanced magneto-capacitance in Sr 2þ modified $BiFeO_3$–$PbTiO_3$ solid solutions, Mater.Chem.Phys.252 (2020) 123313.
39. M. Xu et al., Enhanced energy storage performance of (1-x)(BCT-BMT)-xBFO lead-free relaxor ferroelectric ceramics in a broad temperature range, J. Alloys Compd. 789 (2019) 303–312.